Estimation of power system parameters

Dewi Jones, *Senior Member, IEEE*

***Abstract*—The paper describes the use of a system identification technique to estimate the parameters of a low-order, dynamic model for a power system. The basic technique is to obtain an ARIMAX model by applying a prediction error method to data consisting of 1s samples of the system frequency and the power output of the Dinorwig fast-response pumped-storage station. From this model the natural frequency, damping factor and stiffness (or 'beta') of the power system are obtained. The paper first establishes an appropriate order for the ARIMAX model. Simulation is used to validate the model and ensure that the results are not an artefact of either the input, the identification method or the model structure. It is shown that the precision of the parameter estimates is limited by unknown load disturbances. An example of the use of the technique to analyse the daily variation of parameters is given.**

***Index Terms*— ARIMAX model, power system parameters, system identification.**

I. Introduction

COMMERCIAL pressures, stimulated by de-regulation of electricity markets and the increasing diversity of generation sources (e.g. small-scale distributed generation, wind-power), mean that it is more important than ever to know the dynamic characteristics of a power system. This paper describes how low-order models for a power system can be obtained as 'black box' transfer functions, using a linear system identification method. In particular, estimates of the power system's natural frequency, damping factor and 'grid stiffness' (i.e. the system's power-frequency characteristic, often known as its β value [1]) are obtained. The method takes advantage of the exceptional features of the power that the Dinorwig pumped-storage hydroelectric station contributes to the grid. This station is located in North Wales and is equipped with six 317 MW rated Francis reversible pump-turbines driving synchronous generators, which can be brought from spinning reserve up to full power in 15 s.

Several researchers have considered how to estimate power system characteristics from measured data. Lin et al [2] measure the voltage, frequency and complex power during a rapid, large-amplitude transient caused by a ground fault and obtain a model by means of a least-squares fit of the data to an auto-regressive (AR) difference equation. Similarly, the approach of Inoue *et al* [3] is to fit a polynomial approximation to frequency transients recorded at (unplanned) events on the Japanese power system. Values for the grid's inertia constant and stiffness are estimated for a first-order model of the sort described by Kundur [1]. A planned tripping of a small generator is used by O'Sullivan and O'Malley [4] to produce the frequency and power transients from which the parameters of a first order transfer function are identified. Much work has been done on identifying the parameters of electromechanical oscillations within a power system caused, for example, by energy exchange between generators across transmission lines. A popular method, which appears particularly suited to obtaining the frequency and damping of lightly damped oscillations is Prony analysis, which approximates a transient signal as a weighted sum of damped modal components [5]. Frequency domain approaches have also been considered, such as the procedure proposed by Trudnowski and Donnelly [6] but with the added refinement of a low-level, random probing signal introduced to excite the oscillatory modes of interest. A recent example of on-line estimation is described by Chang-Chien [7] where a moving-average of the β constant of a localised area of the system under automatic generation control (AGC) is found using a recursive least-squares technique. None of the methods cited above yield information about the characteristics of the load imbalance power (ΔP_L). The approach most closely related to this paper is recent work by Wies et al [8], who describe a block processing technique for estimating electromechanical power system modes. They identify an ARMA model for a block of recorded power data, assuming a white-noise input (effectively a special case of the 'disturbance model' referred to in section III) and hence obtain the system's estimated natural frequency and damping factor from the model's dominant pole locations.

The main features which distinguish this work from previous approaches are (a) the use of operational data instead of discrete 'events' involving large system disturbances and (b) use of an ARIMAX (**A**uto **R**egressive **M**oving **A**verage with **I**ntegrator in the noise model and e**X**ogeneous input) structure to model both the input-output relationship and the disturbance due to fluctuating load-generation imbalance. The method takes explicit account of an input, unlike [8] which regards the system output as a time series.

II. System Model and Recorded Data

The model selected to represent the power system is due to Anderson and Mirheydar [9]. Their second order transfer function assumes that the response is dominated by two time constants, one associated with the sum of all the inertias of rotating machines connected to the system and the other with the aggregate effect of all regulatory mechanisms:

D. I. Jones is with the School of Informatics, University of Wales, Bangor, Gwynedd, LL57 1UT, U.K. (dewi@informatics.bangor.ac.uk).

$$\Delta f = \frac{\omega_n^2 T_R}{\beta}\left(\frac{s + 1/T_R}{s^2 + 2\zeta\omega_n s + \omega_n^2}\right)(\Delta P_e - \Delta P_L) \qquad (1)$$

which relates the frequency (Δf) to the power input (ΔP_e) by Dinorwig and the load imbalance power (ΔP_L). In (1) T_R is the effective time constant of all regulatory mechanisms and ω_n, ζ are, respectively, the natural frequency and damping factor; they are functions of T_R and M.

It is shown in [9] that ω_n, ζ and β depend on the droop settings, regulatory time constants and inertia of the plant connected to the power system and are therefore time-varying. The main obstacle to obtaining accurate estimates of these parameters is the continual fluctuation of the unknown load imbalance term, ΔP_L, which largely dominates the changes in system frequency. Here, ΔP_L is regarded as a random disturbance whose characteristics are identified from the recorded data. The ARIMAX model structure allows the parameters of the input-output and disturbance models to be estimated simultaneously. Because the denominator in (1) is common to ΔP_e and ΔP_L, inclusion of the disturbance model aids identification of the input-output model.

The power output of each unit at Dinorwig and the grid frequency are routinely sampled at 1 s intervals and archived. A typical daily record (86400 points) is shown in Figure 1, where the total station power is the sum of the contributions by individual units. The per-unit normalisation is:

$$\Delta P_e(p.u.) = \frac{Power(MW)}{30GW} \qquad \Delta f\,(p.u.) = \frac{freq(Hz) - 50}{50} \qquad (2)$$

The intervals of negative power occur when water is being pumped back to the upper lake, usually at night. Sharp changes in the power flow occur as units are brought on- or off-line. The frequency is a random variable which remains mostly within a band of about ±0.1 Hz of the nominal.

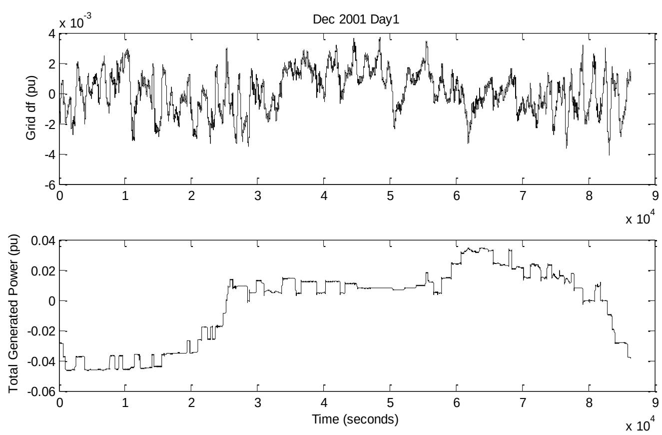

Figure 1 Normalised power-frequency record at Dinorwig.

The power spectral density function of the grid frequency record is shown in Figure 2. Except for the small inflexion in the range 0.3 – 0.4 rad/s, it has a 20dB/decade roll-off with frequency indicating that the frequency variation is essentially a ‘random walk’.

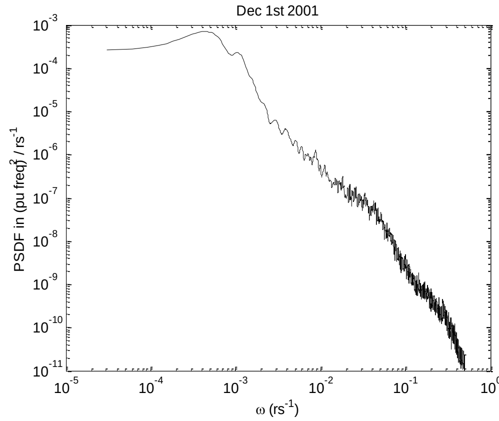

Figure 2 Spectrum of the grid frequency variation for Dec 1st 2001.

Periods of missing data and outliers, caused by instrument malfunction, were located by manual inspection and replaced with linearly interpolated values between reliable data.

III. Parametric System Identification Method

The identification procedure makes extensive use of the powerful prediction-error method described by Ljung [10] and implemented in the Matlab System Identification Toolbox [11]. The transfer function (1) is represented in Figure 3a and in discrete-time in Figure 3b, where $\Delta P_e(k)$ and $\Delta f(k)$ are the system’s measured power input and frequency output at time k, $\Delta P_L(k)$ is the unknown disturbance, q is the forward shift operator and B(q)/A(q) is the system’s time-variant transfer operator. Both ΔP_e and ΔP_L are affected by the grid dynamics, implying that an appropriate black box model should have an equation-error structure [10].

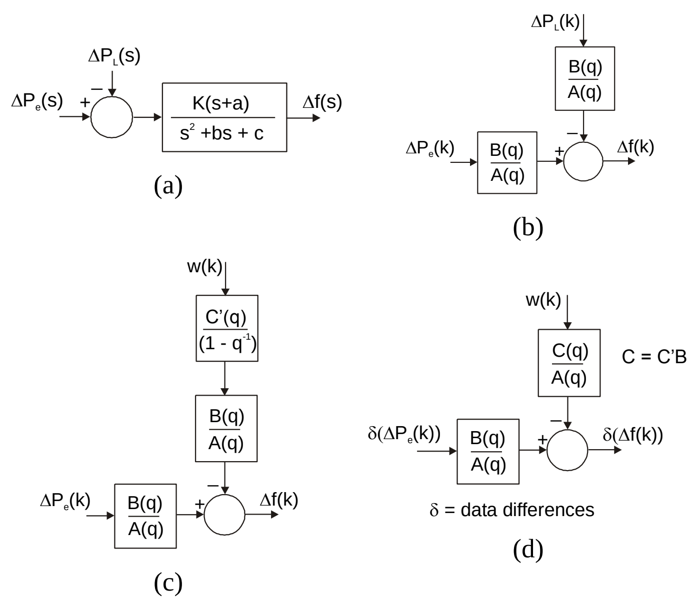

Figure 3 Development of the model structure.

The ‘random-walk’ characteristic of the frequency variation is caused by the load imbalance fluctuation and can be represented as a white noise sequence filtered by an integrator. It is common to include the integrator explicitly in the disturbance model, as shown in Figure 3c, where w(k) is a

Gaussian sequence of independent random variables with zero mean. However, the spectrum of the load imbalance is not necessarily white and this can be accommodated by allowing an extra term C'(q) (whose parameters are to be identified) in the model. Finally, the model is reduced to the ARIMAX form of Figure 3d by working with the differences of the input and output data, $\Delta P_e(k)$ - $\Delta P_e(k-1)$ and $\Delta f(k) - \Delta f(k-1)$. This de-trends the data and focuses the identification process on the higher frequency ranges [10], specifically the range from about 0.01 to 0.1 rad/s in this case. The model structure is therefore:

$$\begin{aligned} \Delta f(k) + a_1 \Delta f(k-1) + \ldots\ldots + a_{n_a} \Delta f(k-n_a) = \\ b_1 \Delta P_e(k-1) + b_2 \Delta P_e(k-2) + \ldots\ldots + b_{n_b} \Delta P_e(k-n_b) + \\ w(k) + c_1 w(k-1) + c_1 w(k-2) + \ldots\ldots + c_{n_c} w(k-n_c) \end{aligned} \quad (3)$$

where $[n_a\ n_b\ n_c]$ determines its order.

$$\text{Let} \quad \begin{aligned} A(q) &= 1 + a_1 q^{-1} + \ldots\ldots a_{n_a} q^{-n_a} \\ B(q) &= \quad b_1 q^{-1} + \ldots\ldots b_{n_b} q^{-n_b} \\ C(q) &= 1 + c_1 q^{-1} + \ldots\ldots a_{n_c} q^{-n_c} \end{aligned} \quad (4)$$

whence : $A(q)\Delta f(k) = B(q)\Delta P_e(k) + C(q)w(k)$ (5)

and : $\underline{\theta} = [a_1 \ldots\ldots a_{n_a} \quad b_1 \ldots\ldots b_{n_b} \quad c_1 \ldots\ldots c_{n_c}]$ (6)

where $\underline{\theta}$ of length ($n_a + n_b + n_c$) is the vector of parameters to be estimated.

Letting $G(q,\underline{\theta}) = \dfrac{B(q)}{A(q)}$ and $H(q,\underline{\theta}) = \dfrac{C(q)}{A(q)}$, then (3) has the general form of a linear system :

$$\Delta f(k) = G(q)u(k) + H(q)w(k) \quad (7)$$

for which the one-step-ahead predictor is given by:

$$C(q)\Delta\hat{f}(k \mid \underline{\theta}) = B(q)\Delta P_e(k) + [C(q) - A(q)]\Delta f(k) \quad (8)$$

where $\Delta\hat{f}(k \mid \underline{\theta})$ is the conditional expectation of y at time k given information up to time (k-1) and noting that $\Delta\hat{f}$ is a function of $\underline{\theta}$. The prediction error is given by :

$$\varepsilon(k,\underline{\theta}) = \Delta f(k) - \Delta\hat{f}(k \mid \underline{\theta}) \quad (9)$$

and the identification method finds the parameter set $\underline{\theta}$ which minimises the criterion:

$$V_N(\underline{\theta}, Z^N) = \frac{1}{N}\sum_{k=1}^{N} \ell\big(\varepsilon_F(k,\underline{\theta})\big) \quad (10)$$

where Z^N is the batch data [$\Delta f(1)$, $\Delta P_e(1)$, $\Delta f(2)$, $\Delta P_e(2)$, ………. $\Delta f(N)$, $\Delta P_e(N)$]. In (10), ε_F is the sequence of prediction errors filtered through a stable linear filter L(q):

$$\varepsilon_F(k,\underline{\theta}) = L(q)\varepsilon(k,\underline{\theta}) \quad (11)$$

and $\ell(\cdot)$ is a scalar valued function. The filter L(q) is used to focus the criterion (10) towards minimising the prediction errors over selected ranges of frequency and can be shown to be identical to changing the disturbance model from H(q, $\underline{\theta}$) to $L^{-1}(q)$ H(q, $\underline{\theta}$). Here, the inclusion of the integrator in the disturbance model, as discussed previously, is formally equivalent to setting L(q) = $(1 - q^{-1})$. The basic choice for $\ell(\cdot)$ is the quadratic norm $\ell(\varepsilon_F) = \varepsilon_F^2/2$ although the algorithm implemented in [11] uses a robust norm [10], designed to limit the influence of occasional outliers in the data set. Adding $[1 - C(q)]\Delta\hat{f}(k \mid \underline{\theta})$ to both sides of (8) and using (9) gives:

$$\Delta\hat{f}(k \mid \theta) = B(q)\Delta P_e(k) + [1 - A(q)]\Delta f + [C(q) - 1]\varepsilon(k,\underline{\theta}) \quad (12)$$

Define the vector of measurements and prediction errors as:

$$\begin{aligned} \phi(k,\underline{\theta}) = [-\Delta f(k-1) \ldots\ldots -\Delta f(k-n_a) \quad \Delta P_e(k-1) \\ \ldots\ldots \Delta P_e(k-n_b) \quad \varepsilon(k-1,\underline{\theta}) \ldots\ldots \varepsilon(k-n_c,\underline{\theta})] \end{aligned} \quad (13)$$

then (12) becomes the pseudo-linear regression [10]:

$$\Delta\hat{f}(k \mid \underline{\theta}) = \phi^T(k,\underline{\theta})\underline{\theta} \quad (14)$$

and, from (9), the prediction errors to be minimised according to criterion (10) are:

$$\varepsilon(k,\underline{\theta}) = \Delta f(k) - \phi^T \underline{\theta} \quad (15)$$

which is done by iterative numerical search using the quasi-Newton or Levenberg-Marquardt algorithms.

IV. Determination of Model Order

The goal here is to obtain the lowest order model which satisfactorily describes the process dynamics. This was done by applying the identification procedure, for various values of $[n_a\ n_b\ n_c]$, to several 90-minute periods from different parts of the data record and observing the step response of the resultant model. The record for the first 90 minute (5400 s) period of Dec 1st 2001 is shown in Figure 4. Dinorwig makes 5 rapid changes of power, of roughly 150 MW magnitude, during this period; their effect on system frequency is easily distinguished. Figure 5 shows the data after differencing.

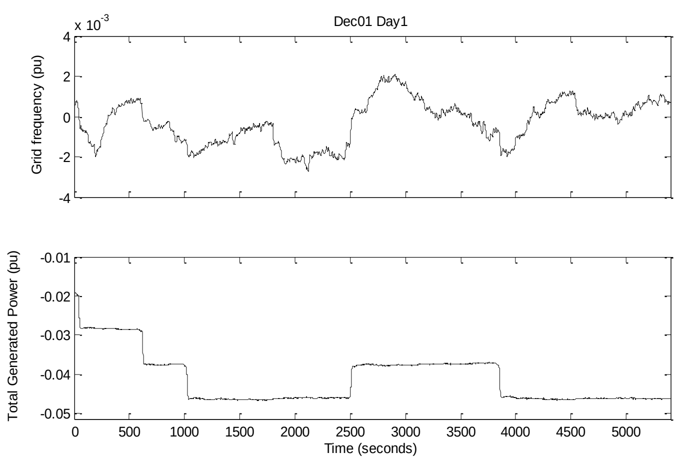

Figure 4 First 5400 seconds of the data record for Dec 1st 2001.

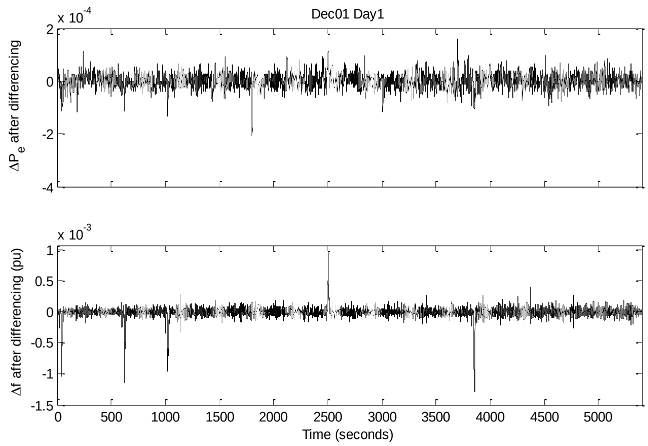

Figure 5 Data for the first period of Dec 1st 2001 after differencing.

Some of the unit step responses for the many models identified from this record are shown in Figure 6 where it is seen that, as the model order increases, there is a convergence towards an underdamped response with a steady state value in the range 0.08 – 0.09. The lower order models tend to give an over-damped response and under-estimate the steady state value while the higher order models exhibit an undesirable high frequency ripple, so a suitable compromise between accuracy and economy in the number of parameters is [n_a = 3 n_b = 2 n_c = 3]. A similar result was obtained using periods from other months in the data record.

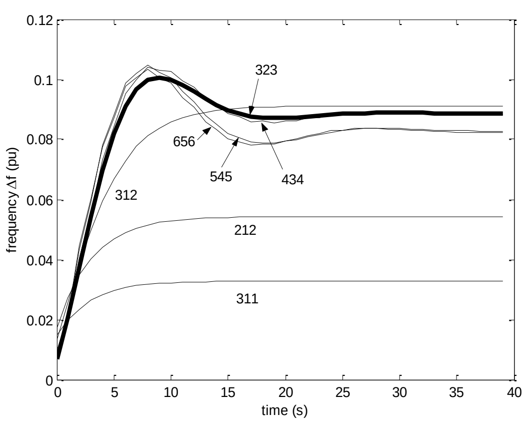

Figure 6 Response of frequency to an unit step in per-unit power for ARIMAX models of various order.

The ARIMAX323 model identified for period 1 is :

$$\begin{aligned}\Delta f(k) &= 1.555\Delta f(k-1) - 0.6607\Delta f(k-2) - 0.00575\Delta f(k-3)\\ &+ 0.00698\Delta P_e(k) + 0.00286\Delta P_e(k-1)\\ &+ w(k) - 0.719w(k-1) - 0.255w(k-2) + 0.281w(k-3)\end{aligned} \quad (16)$$

The discrete transfer function for the input-output part of (16) has the form :

$$\frac{\Delta f(z)}{\Delta P_e(z)} = \frac{z^2(b_0 z + b_1)}{z^3 + a_1 z^2 + a_2 z + a_3} \quad (17)$$

It is possible to reduce (17) to second order and convert it to its continuous form, using standard methods [12], for direct comparison with (3) but inspection of the locations of the poles and zeros shows that this computational step can be avoided. Figure 7a shows the pole-zero maps identified for the sixteen 90-minute periods in the Dec. 1st 2001 record. The most striking feature is the clustering of the dominant poles around ω_n = 0.33 rad/s and ζ = 0.36, which are the values obtained when the whole 24-hour record of Figure 1 is treated as a single data set.

A property of the prediction-error method is that the difference between the estimated parameter values for a record of length N ($\hat{\theta}_N$) and the limit of convergence (θ^*) is asymptotically normal [10]. Thus $(\hat{\theta}_N - \theta^*)$ is a random variable which converges asymptotically to a zero-mean normal distribution of covariance P_θ. Further, $Cov(\sqrt{N}\hat{\theta}_N) \rightarrow P_\theta$ as N→∞ so that the standard deviation of $\hat{\theta}_N$ falls as $1/\sqrt{N}$. An estimate of P_θ may be obtained from the data and used as a confidence interval on the parameter estimates and, hence, the pole and zero locations. The 1σ confidence ellipses for the pole cluster are shown in Figure 7b. These vary in area, depending on the disturbance and the quality of excitation provided by the input during a particular period. The orientation of the major axis also varies, depending on whether the natural frequency or damping factor is considered to be relatively accurate. Decreasing the period in an effort to detect shorter-term power system variation will lead to unacceptable accuracy while increasing the period will decrease uncertainty but at the expense of resolution. This does not, however, mean that the identification technique is not relevant for real-time control purposes as the authors have shown that it can form the basis of a predictive feed-forward controller to improve Dinorwig's frequency-tracking performance.

Another prominent feature of Figure 7a is the cluster of poles near to z = 0 and it is a justifiable approximation to assume that canceling them with zeros at these relatively high frequencies will have little effect on the dominant response. A value for 1/β is easily found from the dc gain of (17) but Figure 7a shows that the behavior of the finite zero in (17) is erratic, which makes evaluation of T_R in (1) unreliable. Sometimes, the pole-zero map for a period deviates from the usual pattern, in which case the dominant pole is selected as the one nearest to the average model for that whole day. Based on this procedure, the parameter values for the first period are ω_n = 0.37 rad/s, ζ = 0.54 and 1/β = 0.089 pu. De-normalising gives β = 674 MW / 0.1 Hz.

The step response $\Delta f / \Delta P_e$ of (16) is shown in Figure 8a, accompanied by a 1σ confidence interval drawn from the asymptotic distribution of the transfer function estimate [10]. Similarly the spectrum of the differenced frequency, when w(k) is white noise, is seen in Figure 8b. Note that the peak of the disturbance spectrum occurs at about 0.3 rad/s, corresponding to the small resonance in Figure 2 that indicates the grid's natural frequency.

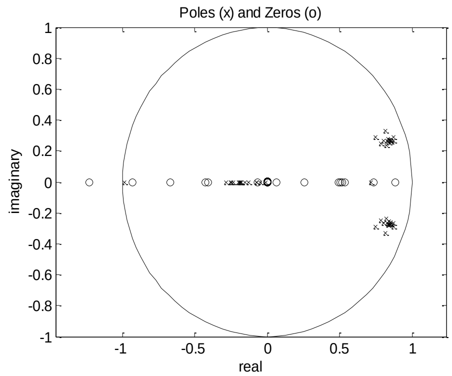

(a)

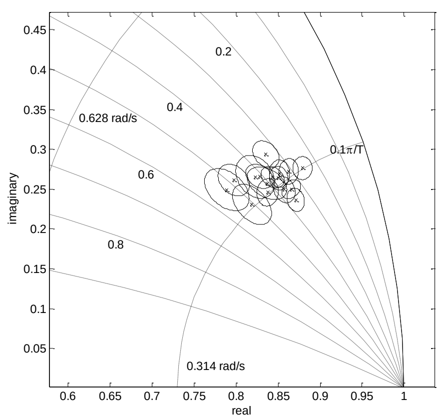

(b)

Figure 7 (a) Pole zero map for the ARIMAX323 models for sixteen 90-minute periods on Dec 1st 2001, (b) the 1σ confidence limits for the pole locations.

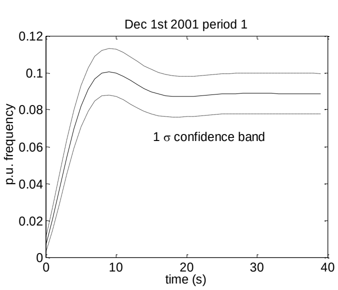

(a)

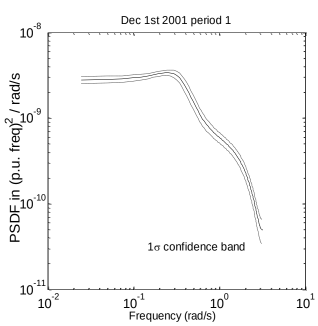

(b)

Figure 8 ARIMAX model for Dec 1st 2001, period 1 (a) step response of input-output model, (b) spectrum of disturbance model (differenced data).

V. VALIDATION

Before applying the identification procedure of section III on a routine basis, it is important to establish how much reliance can be placed on the results. In particular, it is necessary to confirm that the method does extract the properties of the underlying process and that the results are not an artefact of either the input, the identification method or the model structure. A fundamental stipulation is that the input is capable of stimulating the system such that it is identifiable from the output. This is satisfied if the input is 'persistently exciting', i.e. its spectrum $\Phi_u(\omega)$ is different from zero on at least $(n_a + n_b + n_c)$ points in the interval $-\pi < \omega < \pi$. That this is so is illustrated in Figure 9 which shows that the spectrum of the (differenced) input ΔP_e has finite and significant values over the range of frequencies of interest. Specifically, the spectral content over the range 0.1 – 0.5 rad/s is associated with the rapid power changes contributed by Dinorwig (Figure 5) and this makes it particularly useful for identification purposes.

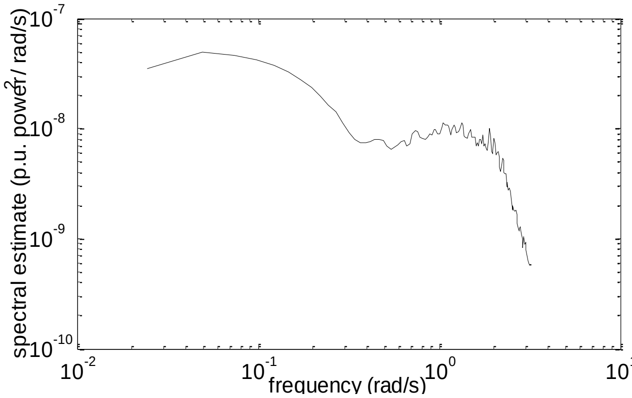

Figure 9 Spectrum of (differenced) power input ΔP_e from Dinorwig for Dec 1st 2001.

It does not, however, guarantee that a good input-output model can be constructed because of the influence of the disturbance ΔP_L. If it is assumed that the linear system (7) has a fixed disturbance model $H(\omega)$ then it is shown in [10] that the minimizing parameter values θ^* can be expressed in the frequency domain as :

$$\theta^* = \arg\min_{\theta} \int_{-\pi}^{\pi} \left| G_0(\omega) - G(\omega,\theta) \right|^2 \frac{\Phi_u(\omega)}{\left| H(\omega) \right|^2} d\omega \qquad (18)$$

where G_0 is the true value of the estimated transfer function G. It is evident from (18) that the quality of the fit of G to G_0 varies with frequency according to the weighting function $\Phi_u(\omega) \,/\, |H(\omega)|^2$. This function can be interpreted as the model's signal-to-noise ratio (SNR), whose magnitude determines the accuracy of the estimation; clearly it is desirable that the spectral content of the input be large compared to the disturbance over the frequency range of interest.

Occasionally, instances occur in the record where the frequency is constant on either side of a rapid power change at Dinorwig, implying that the load disturbance is negligible over this brief interval, and the frequency is responding exclusively to the known power input. An example is the period 615-640 s drawn from Figure 4, which is enlarged in Figure 10. A model was identified from the data for this 25 s interval and used to simulate the frequency change with the measured power as an input. The simulation compares well with the actual frequency as shown in Figure 10. The value of β obtained with the model was 614 MW/ 0.1 Hz compared to 530 MW/ 0.1 Hz calculated manually from the measurements, a 16% difference. Similar spot checks elsewhere in the data record yielded agreement of the β value within 10-20%.

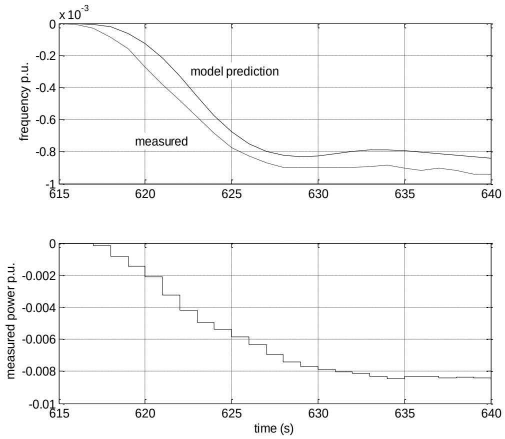

Figure 10 Comparison of measured frequency with the prediction made by the identified model.

Further validation was carried out by simulation which allowed the input and noise sequences and the model to be fixed, so that their individual effect could be assessed. Several cases were considered.

Case 1 : The model (16) was simulated with 5 different input sequences $\Delta P_e(k)$ drawn from other periods of the day. The noise sequence w(k) was fixed at the same unity mean, normally distributed pseudo-random sequence in each case. The identification procedure of section 6 was applied to the simulation's input-output record and the $\Delta f / \Delta P_e$ step responses for the 5 models compared with that of (16). Figure 11 shows that all the responses of the models identified from simulation agree with the original within its 1σ tolerance, indicating that they are not sensitive to the input sequence, i.e. the identified model is not an artefact of the input.

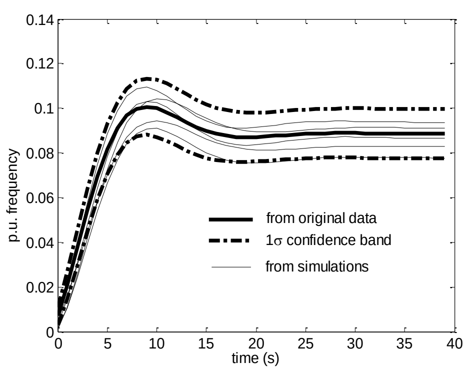

Figure 11 Comparison of the step responses of 5 models identified from simulations with different input sequences and the model identified from the original data.

Case 2 : The model (16) was simulated with 5 different noise sequences w(k) and the same input sequence $\Delta P_e(k)$ and models were identified from the simulation output. Figure 12 shows that the natural frequency and damping of the models identified from simulation agree very well with the original although the steady-state value may vary by up to 20%. This indicates that the identification procedure is not sensitive to the noise sequence although it does emphasize the model variance caused by the rather poor SNR of the data.

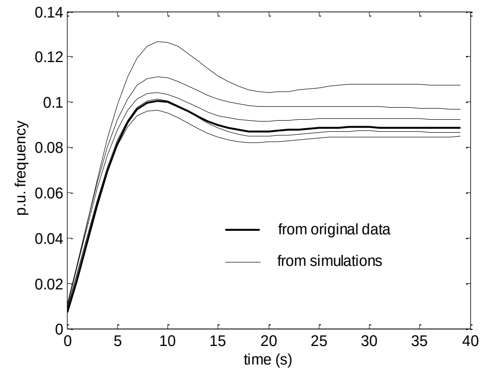

Figure 12 Comparison of the step responses of 5 models identified from simulations with different noise sequences and the model identified from the original data.

Case 3 : Models similar to (16) were identified for periods 4 and 10 (respectively 16,201-21,600 and 48,601-54,000 in Figure 1). These were simulated with ΔP_e from period 1 as input and a fixed noise sequence w(k) and models were identified from the simulation output. Figure 13 shows that, for both periods, there is good agreement between the responses of the models identified from simulation and that identified from the original data, despite the entirely different input and disturbance present in the simulated case.

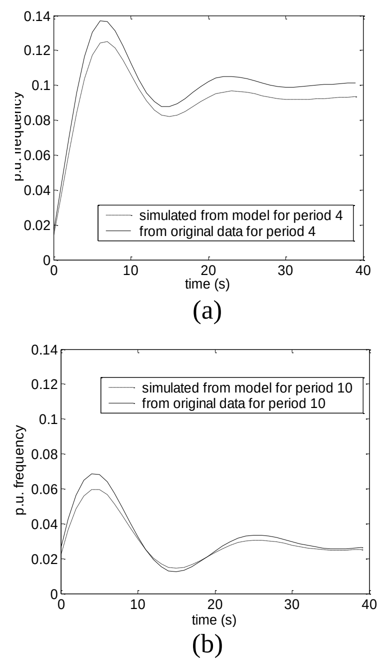

Figure 13 The step responses of 2 models identified from simulations having different input and noise sequences to the data used to identify the original model.

Note that the model identified for period 10 differs significantly from those obtained for the other periods. This does not, however, indicate a true change in the power system. Rather, it occurs because there is no large change in the power input present during period 10 (see Figure 1) i.e. the SNR is particularly low over this period. There is, nevertheless, good agreement between the original model and the one identified from simulated data. These results provide useful validation of the procedure by confirming that the input-output relationship is identified correctly, irrespective of the particular input or disturbance sequences present.

The next stage of validation is to examine whether the identification procedure discerns changes in a model's parameter values and to establish how changes in A(q) and B(q) affect ω_n, ζ and β. The model identified from the complete record in Figure 1, which has the parameter values ω_n = 0.33 rad/s, ζ = 0.36 and $\beta = 645$ MW/ 0.1 Hz (see section IV), was used as a reference. Two noise-free simulations (w(k) set to zero) were performed with the A(q) and B(q) coefficients of this model varied sinusoidally over the day; A(q) was varied by ±10% and B(q) by ±30%. Models were identified for each of the 16 periods in the day and the ω_n, ζ and β parameters derived. The results are shown in Figure 14. Varying A(q) affects all 3 derived parameters and it is clear that a ±10% perturbation changes ω_n and β substantially, with extremum values beyond what is expected during normal operation of the power system. In contrast, the ±30% perturbation in B(q) has a modest effect on the value of β and a negligible effect on ω_n and ζ.

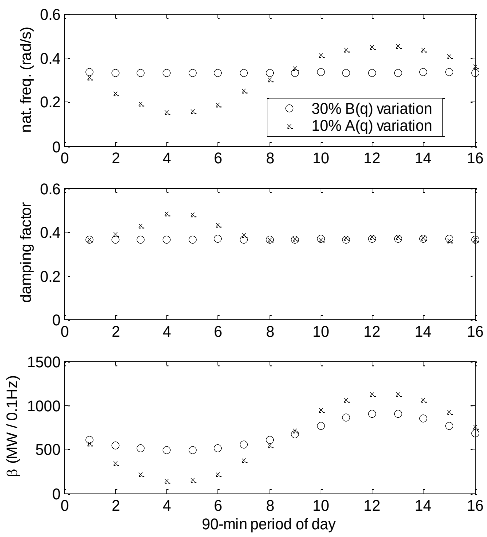

Figure 14 Zero-noise simulation to show the effect of varying A(q) by ±10% and B(q) by ±30%.

The same procedure was repeated, for varying A(q), but with the noise term present. Figure 15 shows how the derived parameters differ from their true values. The value of ω_n agrees well over the whole cycle, except at period 13, while the estimated values of ζ and β generally track the true values but the discrepancies are more pronounced. This is especially true when (as in periods 9 and 10 in Figure 1) there are no substantial changes of power made by Dinorwig. If the simulation is run again but ensuring that a number of input changes occur during every period, the agreement is much better and there is no significant difference between the variances of the three parameters. This emphasizes that the input from Dinorwig is nearer to a filtered piecewise deterministic excitation [13] than a stochastic variable. It seems reasonable that a relationship exists between the accuracy of the estimates and the number and amplitudes of the input changes during a given period, but this has not yet been explored. Overall, it may be concluded that the estimated values of ω_n, ζ and β obtained by means of this identification method are valid measures of the properties of the power system but their precision is limited by the SNR of the data.

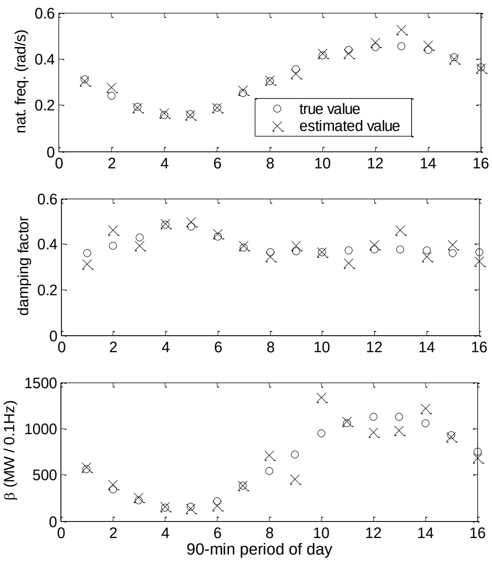

Figure 15 Simulation results comparing the values of the parameters estimated in the presence of noise with their true values.

VI. Results

A typical result of applying the identification method to a daily record, averaged over 1-hour periods, is shown in Figure 16.

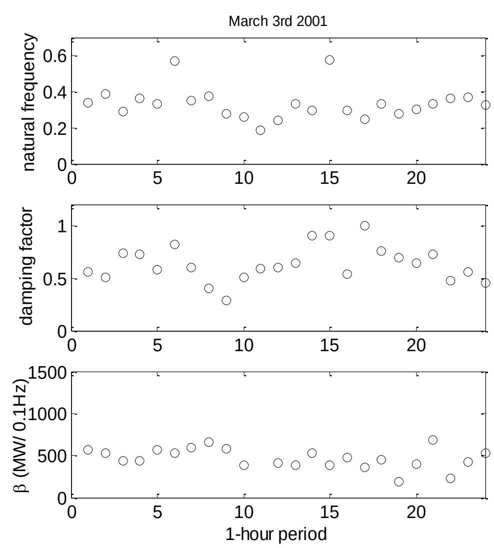

Figure 16 Daily variation of the power system's natural frequency, damping factor and stiffness over a 24 hour period.

The natural frequency generally varies over a narrow range of 0.2 – 0.4 rad/s with little obvious trend, although a slight dip towards the middle of the day is discernible. The two large values at periods 6 and 15 are unreliable because of the absence of Dinorwig input at these times. The damping factor varies widely over the range 0.2 – 1.0 while the stiffness mostly stays between 200 and 700 MW / 0.1 Hz. Overall, the power system's parameters appear to vary over the course of the day with little pattern but within fairly fixed limits.

In order to investigate further whether any recognizable trends exist, the parameter estimates were obtained for each day in the March 2001 record, averaged over 90-minute periods. The results are plotted in Figure 17. Here the wide variation of the individual estimates of all parameter estimates is apparent but taking the median over the month reveals a definite trend. Both the natural frequency and stiffness dip during the daytime from roughly 6am to 6pm while the damping factor tends to increase slightly. This indicates that some statistically significant daily trend in these parameters does exist although the correlation between successive values in the sequence is weak.

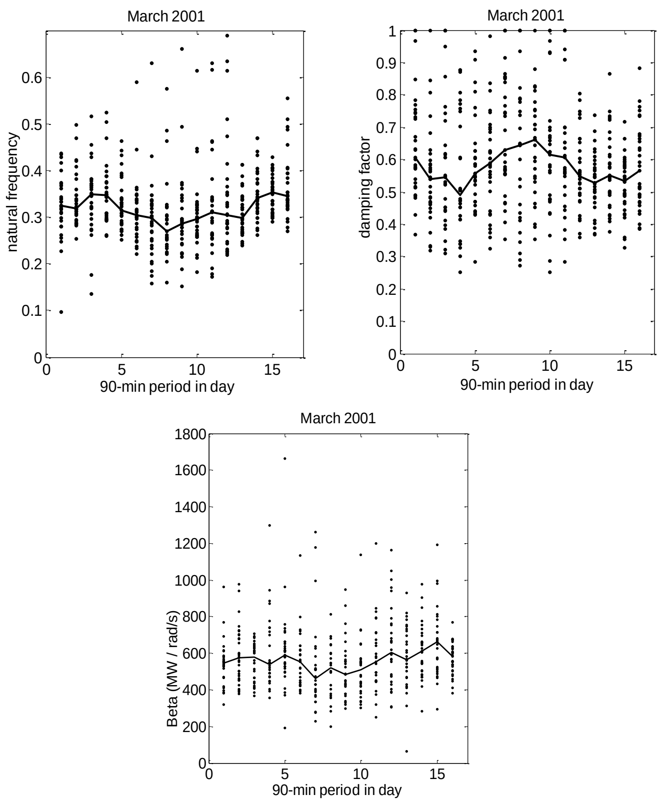

Figure 17 Trends in the median parameter estimates.

VII. Conclusions

Taking advantage of the exceptional form of the output at the Dinorwig power station, this paper has described an identification technique to obtain a low order ARIMAX model for a power system, comprising both an input-output relationship between power and frequency and the spectrum of the disturbance component. Values of the natural frequency, damping factor and stiffness for the power system are derived from the models. Validation by means of simulation shows that the method extracts useful information about the dynamic process but is adversely affected by poor SNR, which inhibits measurement of short-term parameter variations. Applying the method on a systematic basis to the daily record reveals useful information about the expected variation of the parameters. It is currently being used to study parameter variation on the national grid in England and Wales.

VIII. Acknowledgment

The author wishes to thank Arwel Jones and Capell Aris of the First Hydro Company and Sa'ad Mansoor of the University of Wales, Bangor for supplying the data.

IX. References

[1] P. Kundur, *Power System Stability and Control*, Mc Graw Hill, 1994.

[2] C.J. Lin, Y.T. Chen, C.Y. Chiou, C.H. Huang, H.D. Chiang, J.C. Wang and L. Fekih-Ahmed, "Dynamic load models in power systems using the measurement approach." *IEEE Trans Power Systems*, vol. 8(1), pp. 309-315, 1993.

[3] T. Inoue, H. Taniguchi, Y. Ikeguchi and K. Yoshida, "Estimation of power system inertia constant and capacity of spinning-reserve support generators using measured frequency transients", *IEEE Trans Power Systems*, vol. 12(1), pp. 136-143, 1997.

[4] J.W. O'Sullivan, M.J. O'Malley, "Identification and validation of dynamic global load model parameters for use in power system frequency simulations", *IEEE Trans Power Systems*, vol. 11(2), pp. 851-857, 1996.

[5] D.J. Trudnowski, J.E. Dagle, "Effects of generator and static-load nonlinearities on electromechanical oscillations", *IEEE Trans Power Systems*, vol. 12(3), pp. 1283-1289, 1997.

[6] D.J. Trudnowski, M.K. Donnelly, "A procedure for oscillatory parameter identification", *IEEE Trans Power Systems*, vol. 9(4), pp. 2049-2055, 1994.

[7] L. Chang-Chien, N. Hoonchareon, C. Ong and R.A. Kramer, "Estimation of β for adaptive frequency bias setting in load frequency control." *IEEE Trans Power Systems*, vol. 18(2), pp. 904-911, 2003.

[8] R.W. Wies, J.W. Pierre and D.J. Trudnowski, "Use of ARMA block processing for estimating stationary low-frequency electromechanical modes of power systems", *IEEE Trans Power Systems*, vol. 18(1), pp. 167-173, 2003.

[9] P.M. Anderson, M. Mirheydar, "A low-order system frequency response model", *IEEE Trans Power Systems*, vol. 5(3), pp. 720-729, 1990.

[10] L. Ljung, *System Identification - Theory for the User*, 2nd ed, Prentice Hall, 1999.

[11] L. Ljung, *Systems Identification Toolbox v5 - User's Guide*, Natick MA, USA, The MathWorks Inc, 2000.

[12] J.D. Powell, G.F. Franklin and M.L. Workman, *Digital Control of Dynamic Systems*, 2nd ed, Addison-Wesley, 1990.

[13] K. Astrom, B. Wittenmark, *Computer-Controlled Systems*, 3 ed, Prentice Hall, 1997.

X. Biography

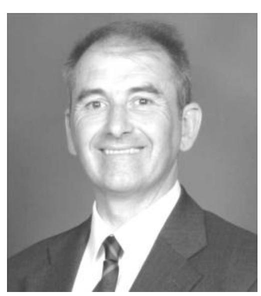

Dewi Jones (M'93, SM'97) received the BSc degree in Electronic Engineering from the University of Wales, Bangor in 1972. The next three years were spent as an Ionosphericist with the British Antarctic Survey after which he returned to the University of Wales, Bangor to take the MSc and PhD degrees in control systems engineering. He then joined the GEC Marconi Research Laboratory in Chelmsford where he worked as a research engineer for two years. In 1980 he was appointed a Lecturer at the University of Wales, Bangor and subsequently became a Senior Lecturer and Reader. From 1994-1996 he was appointed as a Royal Society Industry Fellow and worked for EA Technology Ltd. His main area of interest is control systems applications and he has conducted research into control of electrical and electromechanical devices, real-time parallel computation of control algorithms, vibration isolation for spacecraft, automation of power line inspection and hydroelectric plant control. In 2002, he was awarded the DSc degree by the University of Wales